

You might find this additional information useful...

This article cites 43 articles, 21 of which you can access free at:

<http://jn.physiology.org/cgi/content/full/85/3/1275#BIBL>

This article has been cited by 23 other HighWire hosted articles, the first 5 are:

Neurobiology of a Simple Memory

D. A. Wilson and C. Linster

J Neurophysiol, July 1, 2008; 100 (1): 2-7.

[\[Abstract\]](#) [\[Full Text\]](#) [\[PDF\]](#)

Glutamatergic transmission and plasticity between olfactory bulb mitral cells

D. O. Pimentel and T. W. Margrie

J. Physiol., April 15, 2008; 586 (8): 2107-2119.

[\[Abstract\]](#) [\[Full Text\]](#) [\[PDF\]](#)

Distinct neural mechanisms mediate olfactory memory formation at different timescales

A. M. McNamara, P. D. Magidson, C. Linster, D. A. Wilson and T. A. Cleland

Learn. Mem., February 22, 2008; 15 (3): 117-125.

[\[Abstract\]](#) [\[Full Text\]](#) [\[PDF\]](#)

Dendritic glutamate release produces autocrine activation of mGluR1 in cerebellar Purkinje cells

J. H. Shin, Y. S. Kim and D. J. Linden

PNAS, January 15, 2008; 105 (2): 746-750.

[\[Abstract\]](#) [\[Full Text\]](#) [\[PDF\]](#)

Disynaptic Amplification of Metabotropic Glutamate Receptor 1 Responses in the Olfactory Bulb

D. De Saint Jan and G. L. Westbrook

J. Neurosci., January 3, 2007; 27 (1): 132-140.

[\[Abstract\]](#) [\[Full Text\]](#) [\[PDF\]](#)

Medline items on this article's topics can be found at <http://highwire.stanford.edu/lists/artbytopic.dtl> on the following topics:

Biochemistry .. Aspartate
Neuroscience .. Glutamate
Oncology .. Synaptic Potentials
Physiology .. Dendrites
Physiology .. Smell
Physiology .. Rats

Updated information and services including high-resolution figures, can be found at:

<http://jn.physiology.org/cgi/content/full/85/3/1275>

Additional material and information about *Journal of Neurophysiology* can be found at:

<http://www.the-aps.org/publications/jn>

This information is current as of December 15, 2008 .

Dendritic Glutamate Autoreceptors Modulate Signal Processing in Rat Mitral Cells

PAUL-ANTOINE SALIN,¹⁻³ PIERRE-MARIE LLEDO,³ JEAN-DIDIER VINCENT,³ AND SERGE CHARPAK¹

¹Laboratory of Physiology, Ecole Supérieure de Physique et Chimie, 75005 Paris; ²Centres des Sciences du Goût-Centre National de la Recherche Scientifique, 21000 Dijon; and ³Centre National de la Recherche Scientifique, Institut Alfred Fessard, 91198 Gif sur Yvette, France

Received 19 April 2000; accepted in final form 5 December 2000

Salin, Paul-Antoine, Pierre-Marie Lledo, Jean-Didier Vincent, and Serge Charpak. Dendritic glutamate autoreceptors modulate signal processing in rat mitral cells. *J Neurophysiol* 85: 1275–1282, 2001. It has been shown recently that in mitral cells of the rat olfactory bulb, *N*-methyl-D-aspartate (NMDA) autoreceptors are activated during mitral cell firing. Here we consider in more details the mechanisms of mitral cell self-excitation and its physiological relevance. We show that both ionotropic NMDA and non-NMDA autoreceptors are activated by glutamate released from primary and secondary dendrites. In contrast to non-NMDA autoreceptors, NMDA autoreceptors are almost exclusively located on secondary dendrites and their activation generates a large and sustained self-excitation. Both intracellularly evoked and miniature NMDA-R mediated synaptic potentials are blocked by intracellular bis-(*o*-aminophenoxy)-*N,N,N',N'*-tetraacetic acid (BAPTA) and result from a calcium-dependent release of glutamate. Self-excitation can be produced by a single spike, and trains of spikes result in frequency facilitation. Thus activation of excitatory autoreceptors is a major function of action potentials back-propagating in mitral cell dendrites, which results in an immediate positive feedback counteracting recurrent inhibition and increasing the signal-to-noise ratio of olfactory inputs.

INTRODUCTION

A neuron can synaptically modulate its own output through several mechanisms. First, the axon can establish autaptic contacts on its somato-dendritic compartment (see review by Bekkers 1998; Pouzat and Marty 1998). A second and more common mechanism involves receptors located at the axon terminal. On calcium entry, transmitter is released, activating autoreceptors as well as postsynaptic receptors. In most cases, activation of autoreceptors results in inhibition of transmitter release, although in some cases activation of autoreceptors located at terminals enhances transmitter release (see review by Langer 1997). Finally, a neuron may regulate its firing through the activation of autoreceptors located on the soma and dendrites. These receptors are coupled to G-proteins and mediate a slow autoinhibition. However, recent studies have suggested that in the olfactory bulb, activation of mitral cell dendritic receptors could involve excitatory ligand-gated channels (Aroniadou-Anderjaska et al. 1999; Chen et al. 1998; Isaacson 1999; Salin and Charpak 1998).

Mitral cells (MC) receive olfactory information from sen-

sory neurons and relay it to the cortex after a local processing with olfactory bulb interneurons. MC dendrites are divided into two distinct compartments that are involved in segregated circuits: 1) the primary dendrite that receives hundreds of axonal excitatory terminals from sensory neurons within a given glomerulus and make dendrodendritic synapses with inhibitory periglomerular cells; 2) the secondary dendrites that make dendrodendritic synapses with inhibitory granular cells (Rall et al. 1966) in the external plexiform layer. Both types of dendrites release glutamate and possess a high-density of α -amino-3-hydroxy-5-methyl-4-isoxazolepropionic acid (AMPA), *N*-methyl-D-aspartate (NMDA), and metabotropic glutamate receptors (Montague and Greer 1999; Petralia et al. 1994a,b; van den Pol 1995). However, electron microscopy studies have suggested that excitatory afferent synapses are located exclusively in the distal region of the primary dendrite (Price and Powell 1970). Thus the major part of the mitral cell dendritic arbor is entirely devoid of glutamatergic inputs, although its membrane is provided with glutamatergic receptors. This mismatch has raised the following question: are these dendritic receptors synaptically activated when glutamate is released at and diffuses from the dendrodendritic synapses? It has been shown that the NMDA glutamate autoreceptors of MC dendrites are indeed activated by glutamate released at the dendrodendritic synapses (Aroniadou-Anderjaska et al. 1999; Chen et al. 1998; Isaacson 1999; Salin and Charpak 1998). We show here that, in addition to NMDA receptors, non-NMDA autoreceptors are activated by sodium or calcium spikes, and we analyze the role of self-excitation in the control of MC discharge.

METHODS

Horizontal olfactory bulb slices (300–400 μ m) were obtained from 12- to 22-day-old Sprague-Dawley rats. Self-excitation was also observed in MCs of adult rats (2–5 mo, not shown). Rats were deeply anesthetized with pentobarbital sodium and the brain dissected out in ice cold saline solution (in mM: 124 NaCl, 26 NaHCO₃, 2.5 KCl, 1.25 NaH₂PO₄, 2 Ca₂Cl₂, 1 MgCl₂, and 10 D-glucose saturated with 95% O₂-5% CO₂, pH 7.4). Recordings from mitral cells were performed in an extracellular medium of the same composition as above, using the whole-cell recording configuration with the Axopatch 200A amplifier

Address for reprint requests: P.-A. Salin, CSG-CNRS, Campus Universitaire, 15 rue Hugues Picardet, 21000 Dijon, France (E-mail: salin@cesg.cnrs.fr).

The costs of publication of this article were defrayed in part by the payment of page charges. The article must therefore be hereby marked "advertisement" in accordance with 18 U.S.C. Section 1734 solely to indicate this fact.

(Axon Instruments, Burlingame, CA) in voltage- or current-clamp modes. Recording electrodes were filled with two different types of solution: potassium gluconate solution (120 mM K-gluconate, 10 mM KCl, 2 mM MgCl_2 , 8 mM NaCl, and 10 mM HEPES) and cesium gluconate (in experiments where calcium currents were evoked by a voltage pulse; in mM: 120 Cs-gluconate, 10 CsCl, 2 MgCl_2 , 8 NaCl, and 10 HEPES). Recordings were done at room temperature (22–24°C) and in some cases at 32–34°C. Biocytin (0.5%) or Lucifer yellow (1%) was routinely added to the recording electrode solution to allow morphological identification of the recorded cells. Patch pipettes filled with extracellular solution were used for electrical stimulations (0.1 ms, 10- to 100- μA pulses) of neurons and fibers in the glomerular and external plexiform layers. Inter-trial intervals were 10–20 s. In some experiments, a fine patch pipette was used to selectively section and remove mitral cell axons and dendrites. The following drugs were used: picrotoxin (PTX, Sigma), D-2-amino-5-phosphonovalerate (APV, Tocris), 6-cyano-7-nitroquinolaxine-2,3-dione (CNQX, Tocris), MK-801 hydrogen maleate (MK-801, RBI), 3-[(R)-2-carboxypiperazin-4-yl]-propyl-1-phosphonic acid (CPP, Tocris), tetrodotoxin (TTX, Sigma), 1,2-bis(2-aminophenoxy)ethane-*N,N,N',N'*-tetraacetic acid (BAPTA, Sigma).

RESULTS

MC action potentials, when recorded in control conditions, are followed by a profound synaptic inhibition due to the activation of reciprocal dendrodendritic synapses (Fig. 1*A, left*) (Isaacson and Strowbridge 1998; Jahr and Nicoll 1982; No-

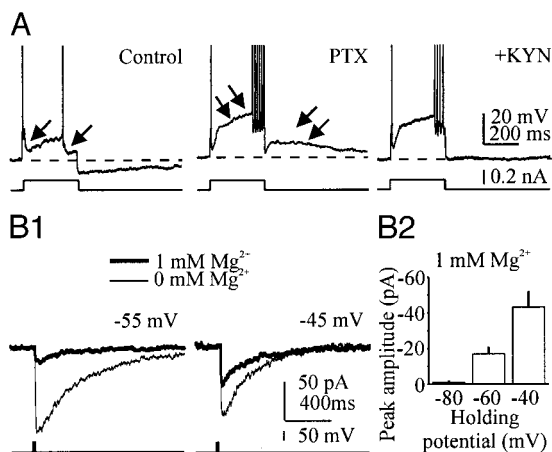


FIG. 1. Blockade of GABA_A receptors unmasks a slow glutamate-mediated excitatory postsynaptic potential (EPSP) in mitral cells. *A*: in control conditions (*left*, current-clamp recording, extracellular magnesium: 1 mM, V_h : -62 mV), an action potential triggered a strong recurrent synaptic inhibition (arrow) that was blocked during bath application of the GABA_A receptor antagonist picrotoxin (PTX, 100 μM , *middle*). Note that the blockade of inhibition unmasks a slow depolarizing afterpotential (DAP, double arrow) during which the cell fires. Subsequent application of the nonselective ionotropic glutamate receptor antagonist kynurenic acid (KYN, 10 mM) strongly reduced the slow DAP, which thus corresponds to a slow-EPSP (*right*). The bottom lines indicate the depolarizing current pulses. *B1*: voltage-clamp recordings (averages of 5) of the *N*-methyl-D-aspartate (NMDA) current underlying the slow-EPSP. A single sodium spike induced an inward current that was reduced in the presence of magnesium [100 μM PTX and 20 μM 6-cyano-7-nitroquinolaxine-2,3-dione (CNQX); averages of 5]. The D-APV-sensitive component of the slow excitatory postsynaptic current was voltage dependent, being reduced at hyperpolarized potentials when the recording was done in the presence of magnesium (1 mM). The evoked Na currents were digitally removed. The bottom lines indicate the voltage steps. *B2*: summary graph illustrating the voltage dependency of the D-APV-sensitive component of the slow synaptic current recorded in the presence of magnesium (100 μM PTX and 10–20 μM CNQX). The abscissa shows the holding potential of the cell and the ordinate the maximum peak amplitude. The error bars indicate SE.

wycky et al. 1981a; Rall and Shepherd 1968; Schoppa et al. 1998). In the presence of GABA_A receptor antagonists, a slow depolarizing afterpotential (DAP) was unmasked (Fig. 1*A, middle*) (Aroniadou-Anderjaska et al. 1999; Isaacson 1999; Nicoll and Jahr 1982; Nowycky et al. 1981b). DAP was abolished by kynurenic acid, a non-selective ionotropic glutamate receptor antagonist (Fig. 1*A, right*), suggesting that it did not result from the activation of intrinsic membrane properties but rather that it was a slow glutamate-mediated excitatory postsynaptic potential (slow-EPSP). In voltage-clamp conditions (Fig. 1*B1*), voltage steps evoking partially clamped sodium spikes evoked slow inward synaptic currents underlying the slow-EPSP. In the absence of extracellular Mg^{2+} , the slow current was strongly enhanced (Fig. 1*B1*). In the presence of 1 mM Mg^{2+} , the current underlying the slow-EPSP displayed a rectification at hyperpolarized potentials typical of an NMDA current blocked by magnesium (Fig. 1, *B1* and *B2*).

In contrast to a recent study (Isaacson 1999), we found that the slow current presented two components: a major one sensitive to the NMDA receptor antagonists D-APV (25–100 μM) and CPP (10–20 μM) and a second one sensitive to the non-NMDA receptor antagonists CNQX (10–20 μM) and 2,3-dioxo-6-nitro-1,2,3,4-tetrahydrobenzoquinolaxine-7-sulphonamide (NBQX) (10 μM ; Fig. 2, *A* and *B1*). About 20% of the total current recorded in absence of Mg^{2+} was blocked by CNQX (Fig. 2*B1*; 28.5 ± 7 pA vs. 136.8 ± 36.4 pA, mean \pm SE, $n = 10$, $P = 0.01$, Student's *t*-test). The broad spectrum metabotropic glutamate receptor antagonist (S)- α -methyl-4-carboxyphenylglycine (MCPG) (0.5–1.5 mM) had no effect (Fig. 2*B1*). The non-NMDA-mediated current, although slow, was faster than the decay of the NMDA-mediated component (AMPA/kainate-R component: 58.6 ± 11.3 ms, $n = 6$ vs. NMDA-R component: 230.1 ± 25.1 ms, $n = 7$, $P = 0.0001$; Fig. 2*B2*).

To test whether this phenomenon was a self-excitation due to the activation of MC glutamatergic autoreceptors, we considered and eliminated a variety of other potential synaptic mechanisms. The slow-EPSP could be due to a recurrent excitation since excitatory synaptic contacts impinging on MCs have been observed (Martinez and Freeman 1984; Nicoll 1971; Nowycky et al. 1981b). Action potentials (Bischofberger and Jonas 1997; Chen et al. 1997; Isaacson and Strowbridge 1998) initiated or backpropagating in dendrites could thus activate periglomerular and/or external plexiform excitatory cells via dendritic release sites (Fig. 3, *top*). We thus used focal electrical stimulations to activate neurons or fibers in the glomerular and external plexiform layers. Extracellular electrical stimulations generated large EPSCs in mitral cells that were reduced in the presence of (2*S*,2'*R*,3'*R*)-2-(2',3'-dicarboxycyclopropyl)glycine (DCGIV), an agonist of group II metabotropic glutamate receptors (Fig. 3*A1*). As in other regions of the brain (Kamiya and Ozawa 1999; Macek et al. 1996; see for review: Conn and Pin 1997), DCGIV acted presynaptically by inhibiting glutamate release as suggested by the switch from paired-pulse depression to paired-pulse facilitation of the response (Fig. 3, *A1* and *A2*). While DCGIV (10 μM) strongly decreased the size of the extracellularly evoked EPSP (Fig. 3*B1*, $79 \pm 5.7\%$ of decrease, $n = 12$ cells in 7 slices, 13 sites of electrical stimulation located in the glomerular layer and 12 sites of electrical stimulation located in the external plexiform layer), it did not reduce the amplitude of the slow-EPSP (Fig.

3B2) generated in the same mitral cells. Thus it is unlikely that olfactory bulb excitatory fibers, which are inhibited by DCGIV, play a role in the generation of the slow-EPSP.

Another possibility was that MCs establish autaptic excitatory synapses since they send axonal collaterals in the external plexiform layer, which also contains their secondary dendrites (Fig. 3, top). Autapses have recently been shown to be functional in the CNS (Pouzat and Marty 1998). We found that when MCs were recorded in voltage-clamp conditions with a cesium-gluconate containing pipette, the inward current following a mixed sodium/calcium spike (partially clamped) decreased by only $6.5 \pm 2.6\%$ ($n = 6$) in the presence of tetrodotoxin (TTX, Fig. 3C, 1 μ M), a finding previously reported (Isaacson 1999; Nicoll and Jahr 1982), suggesting that sodium spikes are not a prerequisite for the induction of the slow synaptic response. The role of an autaptic connection mediated by a calcium spike propagation was further excluded

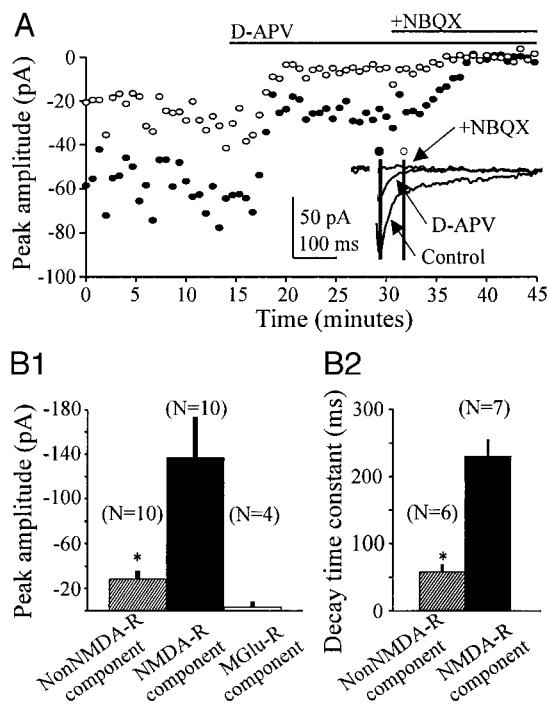


FIG. 2. The slow glutamate-mediated excitatory postsynaptic current has 2 components. **A:** voltage-clamp recordings ($V_h = -70$ mV) of the current underlying the slow-EPSP. Time course amplitude of the fast (●, see inset) and of the slow (○) component of the inward current recorded in the absence of extracellular magnesium and with PTX. A single sodium spike induced an inward current that was reduced by the successive application of D-APV (100 μ M) and of D-APV (100 μ M)-2,3-dioxo-6-nitro-1,2,3,4-tetrahydrobenzoquinoline-7-sulphonamide (NBQX) (10 μ M). **B1:** summary graph of each glutamatergic receptor-mediated component contributing to the slow excitatory postsynaptic current. Peak values were obtained after subtraction of the currents recorded in the presence of 10–20 μ M CNQX (7 cells or 10–20 μ M NBQX, in 3 cells), 50–100 μ M D-APV [6 cells or 10–20 μ M 3-(R)-2-carboxypiperazin-4-yl]-propyl-1-phosphonic acid (CPP) in 4 cells] and 0.5–1.5 mM (S)- α -methyl-4-carboxyphenylglycine (MCPG) (4 cells), respectively, from the control current peak values. After the subtraction, the maximum peak currents represented in the bar graph were calculated as in **A** (see ● and the 1st vertical bar). Calculations of the peak currents were done at least 10 min after the beginning of application of the antagonists (average of 5–10 traces). Note that in average the NMDA-R component represents more than 80% of the total current. MCPG exerted no action on the slow excitatory EPSC, suggesting that mGluR-mediated response does not contribute to the slow-EPSP. **B2:** summary graph of the decay time constant of the NMDA-R and non-NMDA-R currents (recordings in 0 mM magnesium and with PTX).

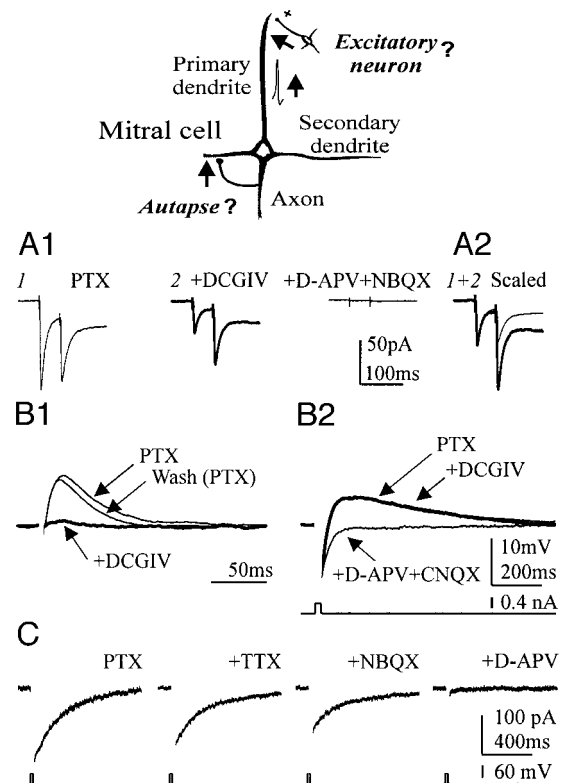


FIG. 3. Excitatory connections sensitive to group II metabotropic glutamate receptor agonists and autapses do not play a role in the genesis of the slow EPSP. **Top:** schematic diagram illustrating 2 hypotheses that may explain self-excitation: 1) the action potential backpropagating in the primary dendrite activates a disynaptic excitatory circuit in the olfactory bulb; 2) the action potential activates an axo-dendritic autapse. **A1:** (2S,2',R,3',R)-2-(2',3'-dicarboxycyclopropyl)glycine (DCGIV), a group II metabotropic glutamate receptor agonist, inhibited excitatory responses evoked by focal electrical stimulation of the olfactory bulb superficial layers. **Left:** voltage-clamp recording (averages of 10 traces, K-gluconate-filled patch pipette) of an EPSC evoked by an extracellular stimulation of the glomerular layer with a patch pipette filled with the extracellular solution (PTX and Mg^{2+} , 1 mM). **Middle:** low concentration of DCGIV (1 μ M) reduced the size of the evoked inward current. No steady-state current was observed during the application of DCGIV. **Right:** the application of the ionotropic glutamate receptor antagonists D-APV (50 μ M) and NBQX (10 μ M) totally abolished the evoked EPSC. **A2:** the average traces of the recording made in the presence of picrotoxin (thin line, 1) and with the addition of DCGIV (thick line, 2) are scaled with the 1st response. The change from paired-pulse depression to paired-pulse facilitation suggests that DCGIV acts presynaptically. **B1:** an EPSP (averages of 10 traces) was evoked in a mitral cell in response to an electrical stimulation applied focally in the external plexiform layer. DCGIV (10 μ M) deeply reduced the amplitude of the excitatory response. **B2:** in contrast, DCGIV had no effect on the slow-EPSP recorded in the same cell, indicating the involvement of 2 different mechanisms in the generation of these EPSPs (the extracellular solution contained PTX and Mg^{2+} , 1 mM). The evoked sodium current was digitally removed. **C:** the suppression of sodium spikes does not block the slow-EPSC. Voltage-clamp recordings were performed with a patch pipette containing cesium gluconate ($V_h = -70$ mV). In control (PTX), a 60-mV voltage step evoked a sodium current associated with a calcium current (truncated) followed by a slow-EPSC. Tetrodotoxin (1 μ M) and then the non-NMDA receptor antagonist NBQX (10 μ M) reduced the size of the inward current, which was then completely abolished by D-APV (50 μ M); $Mg = 0$ mM.

by experiments where the MC axon was sectioned from the soma before the recording ($n = 5$, data not shown) without blocking the slow synaptic response. Both NMDA-R and AMPA/kainate-R currents persisted in these recording conditions. Altogether, these results exclude autaptic connections as a mechanism for the genesis of the slow-EPSP.

In MCs, self-excitation could occur either at dendritic release sites located on the glomerular tuft or on secondary dendrites since backpropagating action potentials reach both levels of the dendritic tree (Bischofberger and Jonas 1997; Chen et al. 1997; Isaacson and Strowbridge 1998). The glomerular layer was completely removed (before recording) in a first set of experiments. Figure 4 indicates that, in the absence of the distal primary dendrite, MCs still presented a prolonged inward current due to the activation of ionotropic glutamate receptors. Additional experiments showed that MCs without distal primary dendrites consistently displayed slow-EPSPs with large amplitudes (4.8 ± 1.2 mV, $n = 6$ vs. 5.7 ± 0.7 mV in control, $n = 7$, $Mg^{2+} = 0$ mM).

In another series of experiments, we quantified the contribution of both dendritic compartments by comparing the amplitude of the slow-EPSP before and after section (with a gentle suction) of the apical primary dendrite. The dendritic section abolished the olfactory nerve-evoked EPSPs ($n = 3$). We analyzed the effect of dendritic removal on the amplitude of both the NMDA- and non-NMDA components of the slow-EPSP. We found that the amplitude of the non-NMDA component significantly decreased after suppression of the primary dendrite (Fig. 5, *A1* and *A2*; $44.2 \pm 10.1\%$, $n = 6$). However, the major component of the slow-EPSP (i.e., the NMDA one) was almost unaffected (an average decrease of $9.3 \pm 1.6\%$, $n = 6$). As shown on Fig. 5*B2*, the section of the apical primary dendrite did not modify significantly the input resistance and the resting membrane potential in the same MCs. This rules out that a significant decrease of the NMDA response was covered by an increase in the space constant. Altogether, these results suggest that action potentials backpropagating in the primary dendrite activate primarily non-NMDA autoreceptors while those backpropagating in secondary dendrites activate mainly NMDA autoreceptors.

In secondary dendrites, the slow-EPSP could result from the activation of dendrodendritic synapses established between a MC and another excitatory connection insensitive to DCGIV but also from the activation of MC ionotropic glutamate auto-

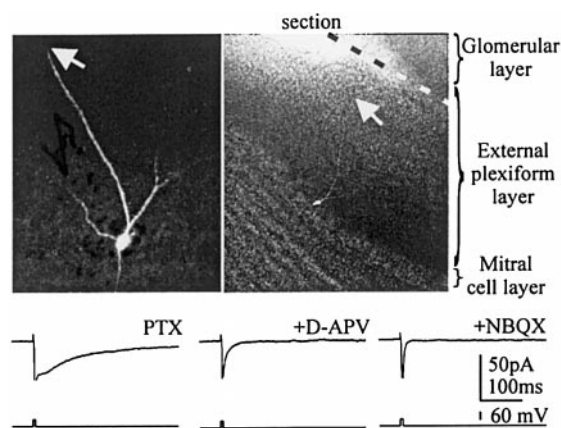


FIG. 4. The slow-EPSP persists in the absence of the apical tuft. *Top left*: picture of a mitral cell labeled by Lucifer yellow. Note the absence of the distal part of the primary dendrite. *Top right*: location of the labeled mitral cell in the olfactory bulb. The section of the superficial external plexiform layer was made immediately after cutting the slice with a small piece of razor blade and under the control of a microscope. The single arrow shows the end of the primary dendrite. *Bottom*: most of the slow-EPSC recorded in the illustrated mitral cell was blocked in the presence of D-APV (voltage clamp, K-gluconate, average of 15 traces, $Mg^{2+} = 1$ mM).

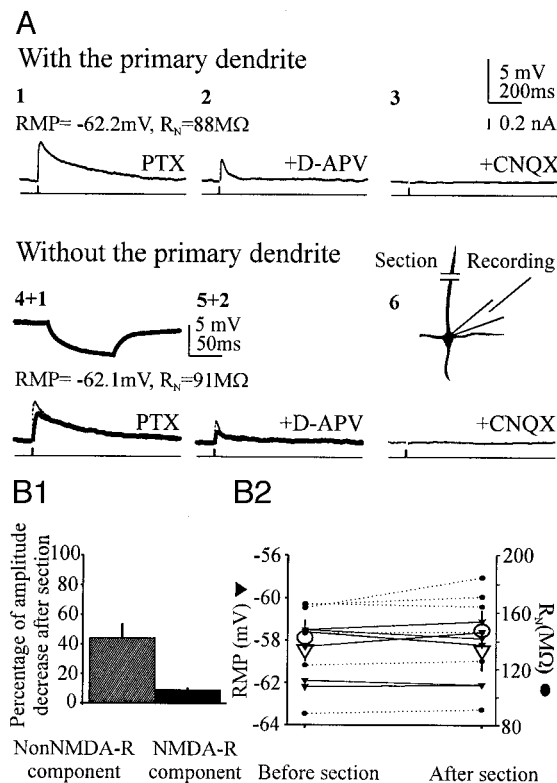


FIG. 5. NMDA receptors of the secondary dendrites mediate the major component of the slow-EPSP. *A1*: respective contribution of both dendritic compartments to the slow-EPSP. The slow-EPSP was recorded in control conditions ($Mg^{2+} = 1$ mM, PTX, 100 μ M), then in the presence of D-APV (50 μ M), D-APV, and CNQX (5 μ M), and finally back in control conditions (*top*, 3 average traces of 10 responses). In a 2nd step, the apical primary dendrite was sectioned with a gentle suction under visual control, and the slow-EPSP was again recorded in the 3 conditions [*bottom*, 3 dark traces that are the average of 10 responses; light traces are the average responses with the primary dendrite (in 1 and 2)]. The dendritic sectioning of the recorded neuron was relatively easy because the primary dendrites were very well defined under the microscope. The sectioning of the primary dendrite had a small effect on the slow-EPSP (see 4 + 1; *bottom left traces*). Note that this small decrease in the slow-EPSP is mainly due to a decrease in the non-NMDA-R-mediated component (see the 2 superimposed traces 5 + 2, *bottom middle traces*). *Inset*: superimposed average traces (20 traces) of the cell membrane potential before (thin line) and after (thick line) sectioning to illustrate the absence of input resistance change. *B1*: summary graph showing the percentage of the NMDA and the AMPA components of the slow-EPSP before and after section of the apical dendrite. Note that the NMDA component was only slightly modified by the sectioning. The measurements of the slow-EPSP were done 10 min after the beginning of the application of the glutamate receptor antagonists. The following concentrations of the receptor antagonists were used in these series of experiments: D-APV (25–50 μ M), CNQX (5–10 μ M). *B2*: the sectioning of the apical primary dendrite has no significant effect on the input resistance (R_{in}) and the resting membrane potential (RMP). The quantification of the input resistance immediately before and after the section of the apical dendrite does not show a significant increase (141.6 ± 12.7 vs. 147 ± 13.9 M Ω , $P = 0.17$, paired t -test, $n = 6$, analysis done with the cells illustrated in *B1*). No modification of the membrane resting potential was observed during this manipulation (60.5 ± 0.8 vs. 60.5 ± 0.5 mV, $n = 6$).

receptors by glutamate released from the dendrites. If the latter hypothesis were true, the slow-EPSP should be observed in conditions where the entire olfactory bulb network is uncoupled. In the presence of PTX, CNQX, TTX, and extracellular Mg^{2+} (2 mM), there were no synaptic interactions between cells at rest (the resting membrane potential was about -80

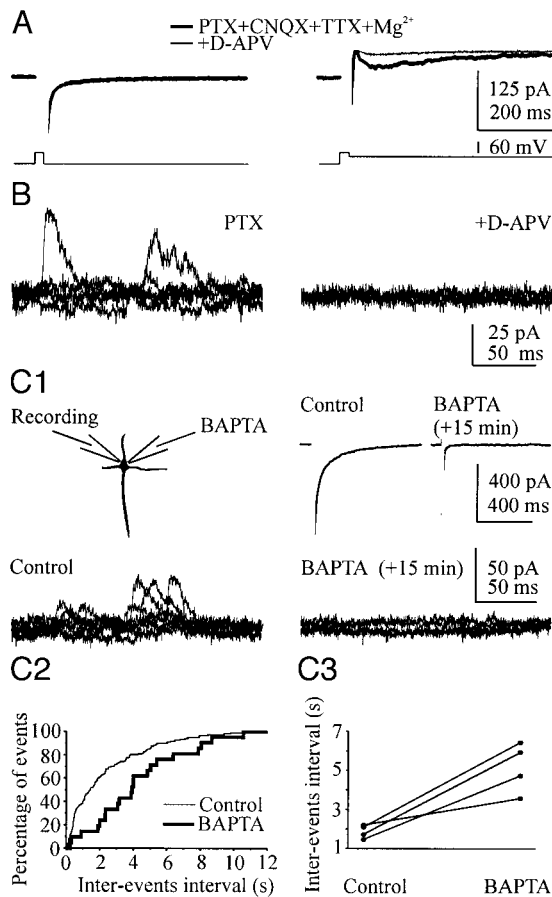


FIG. 6. NMDA autoreceptors mediate MC's self-excitation. **A**: glutamate released by secondary dendrites activates NMDA autoreceptors in an uncoupled network. In the presence of Mg^{2+} (2 mM), PTX (100 μ M), TTX (1 μ M), and CNQX (20 μ M), evoking a calcium current did not induce any slow inward current when the membrane potential was voltage clamped at -80 mV (*left*). In contrast, when the membrane was depolarized to -40 mV, to relieve the magnesium block, the NMDA component of the slow excitatory postsynaptic current was revealed (*right*). **B**: NMDA autoreceptors mediate miniature synaptic currents. At a holding potential of $+40$ mV and in the presence of tetrodotoxin (1 μ M), outward synaptic events were recorded (*left*) and could be blocked by 50 μ M D-APV (*right*). Note the absence of D-APV-insensitive spontaneous outward currents. **C1**: in another cell, NMDA miniature synaptic currents were first recorded in the same conditions (*bottom left*). After 10 min, an additional patch pipette containing the calcium chelator BAPTA (20 mM) was used to record the same cell. Fifteen minutes after the intracellular application of BAPTA, the slow inward current evoked by a calcium current totally disappeared (*top right*, $V_h = -70$ mV). In the same cell, the frequency of spontaneous synaptic events also decreased (*bottom right*) after this manipulation, suggesting that they were generated, at least in part, by a direct activation of NMDA autoreceptors by glutamate released from the recorded MC ($V_h = +40$ mV). **C2**: cumulative distribution of NMDA miniature events recorded in a MC in control (thin line) and in the presence of BAPTA (thick line) after 15 min (2.379 ± 2.41 s vs. 4.2 ± 0.624 s, $P = 0.0002$; nonparametric Kolmogoroff-Smirnov test). **C3**: summary graph of the inter-event interval in control and in BAPTA for 4 MCs (means of 2.03 ± 0.26 s and 5.1 ± 0.64 s, respectively, $P = 0.004$, paired t -test). Picrotoxin (100 μ M) was applied in all experiments.

mV). Evoking a calcium current in a MC in these conditions did not induce any synaptic component (Fig. 6A, *left*). However, when the membrane potential of the stimulated cell was depolarized to -40 mV, to relieve the Mg^{2+} block, the NMDA current was revealed (Fig. 6A, *right*). These results strongly suggest that NMDA autoreceptors mediate self-excitation in secondary dendrites.

The NMDA autoreceptors are also spontaneously activated in conditions of minimal glutamate release. In the presence of PTX, TTX, and in the absence of extracellular Mg^{2+} , the membrane potential of MCs was clamped at $+40$ mV. NMDA-mediated miniature synaptic potentials could then be recorded (Fig. 6B). These events did not result from the activation of NMDA receptors by ambient glutamate. Indeed, when a second patch pipette was then used to inject the calcium chelator BAPTA (Fig. 6, C1 and C2, *bottom*) in the same cell, the frequency of spontaneous NMDA synaptic currents progressively diminished after breaking the membrane seal. Concurrent with the decrease in spontaneous miniature synaptic potentials, the current underlying the evoked slow-EPSP at -70 mV was progressively blocked (Fig. 6C1, *top right*) as BAPTA slowly diffused to dendritic release sites (Adler et al. 1991; Borst and Sakmann 1996). Fifteen minutes after the seal break, the inter-event interval had increased from 2.03 ± 0.26 s to 5.1 ± 0.64 s ($P = 0.004$, $n = 4$, paired t -test, Fig. 6C3) while the amplitude of NMDA miniature currents had not changed (13 ± 2.4 pA vs. 10.9 ± 1.1 pA, $n = 4$, $P > 0.5$).

To understand the functional role of the slow-EPSP, we examined its dynamic properties. Figure 7A illustrates that there was a temporal summation of the slow-EPSP with an increase in cell firing. Paired-pulse facilitation occurred when two sodium action potentials were separated by <300 ms, and was maximal at an inter-spike interval of approximately 50 ms (Fig. 7, B and C). Given that, during odor stimulation, MCs fire in a range close to this interval (Wellis et al. 1989), it is likely that self-excitation significantly contributes to the mitral cell's response.

To demonstrate this, we tested the role of NMDA autoreceptors on MC discharge. Given that the dendrodendritic inhibition is entirely dependent on the glutamate ionotropic receptor activation (Isaacson and Strowbridge 1998; Schoppa et al. 1998), the use of extracellularly applied glutamate receptor antagonists may result also in an important effect on MC firing by a blockade of the disynaptic inhibition. Thus to address the issue of the physiological role of self-excitation, it was necessary to block synaptic inhibition prior to test the effect of NMDA receptor antagonists. In the presence of PTX, CNQX, and extracellular Mg^{2+} (and in 3 cases after a cut of the primary dendrite), a train of action potentials was regularly evoked with a current depolarizing step (Fig. 8A1). During the mitral cell discharge, NMDA autoreceptors were activated. After having established a stable baseline of the cell discharge, we applied the NMDA receptor antagonists MK801, D-APV, or CPP. The NMDA open channel blocker MK801 modestly, but significantly, increased the average inter-spike interval (19.8 ± 1.8 ms vs. 23.3 ± 2.3 ms for the 3rd inter-spike interval, $n = 6$, $P = 0.0125$, paired t -test, 4 cases in 1 mM Mg^{2+} and 2 cases with 0.8 mM Mg^{2+}) in a use-dependent manner (Fig. 8A2). Application of the competitive NMDA receptor antagonists D-APV (50 μ M) and CPP (10 μ M) had also similar effects (20.3 ± 1.3 ms vs. 25.1 ± 2.1 ms, $P = 0.008$, $n = 4$). The protocol used here evoked trains of several action potentials that may activate numerous surrounding mitral cells (i.e., Isaacson 1999). Thus the application of competitive NMDA antagonists may overestimate the real contribution of NMDA autoreceptors on the MC's excitability. In contrast, the activity-dependent blocker

MK801 inhibited the NMDA autoreceptors activated by the glutamate release from the recorded cell and not all NMDA receptors present in the network. As shown in Fig. 8A1, the first spike of the discharge was exactly superimposed in control (with PTX) and in MK801 conditions, indicating that the blockade of the effect of ambient glutamate (Sah et al. 1989) did not produce a large change in the membrane resting potential (Fig. 8B1) and in the spike threshold (Fig. 8B2). For different values of depolarizing current, the latency of the first spike was also the same in control conditions and in the presence of MK801. Moreover, in the entire population of cells analyzed here, the latency of the first spike after an application of the NMDA-R antagonists was not modified. As a result, the average spike frequency for each cell decreased after application of MK801, although the spike threshold was not modified (Fig. 8A3, left). Figure

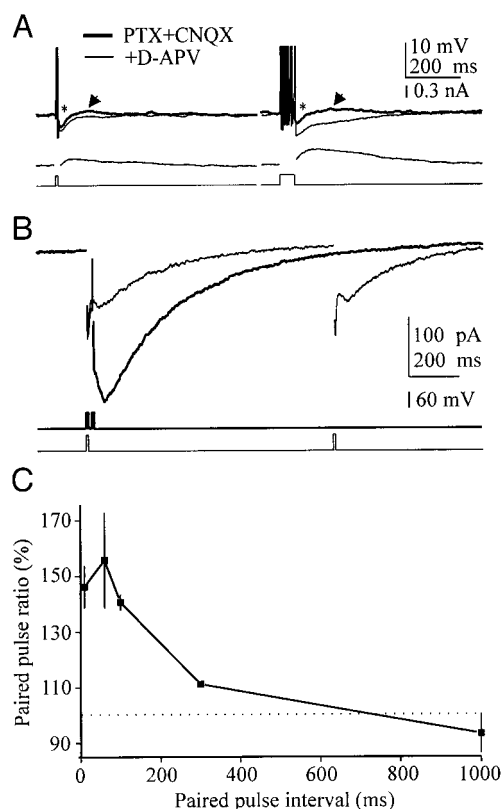


FIG. 7. Short-term facilitation of self-excitation by mitral cell's action potentials. A: the size of the slow-EPSP is modulated in an activity-dependent manner. Top: the slow-EPSP (arrow) increases with the number of spikes (1 on the left, 4 on the right; thick lines, V_h : -59 mV). Application of glutamate receptor antagonists blocked the slow-EPSP (thin lines) and revealed the afterhyperpolarization (star) entirely. Bottom: the traces (averages of 10) represent the difference between traces obtained in control (100 μ M PTX, 20 μ M CNQX, Mg^{2+} = 1 mM) and with the addition of the NMDA antagonist D-APV (50 μ M). The sodium spikes are digitally removed. B: paired-pulse facilitation of the current underlying the slow-EPSP. Top: a mitral cell was voltage-clamped at -70 mV (K-gluconate) and 2 voltage steps (2 ms, 60 mV) were applied successively, separated by either 30 ms (thick line) or 1 s (thin line). The 2nd slow-EPSC clearly increased when the inter-pulse interval was brief (30 ms). The extracellular solution contained 100 μ M PTX and 20 μ M CNQX (Mg^{2+} = 0). The evoked sodium currents were digitally removed. C: summary graph showing that paired-pulse facilitation lasts up to 300 ms (n = 5 cells). The paired-pulse ratio was calculated as the ratio of the amplitudes of the 2nd slow-EPSC over the 1st slow-EPSC. The dash line indicates a paired-pulse facilitation ratio of 100%.

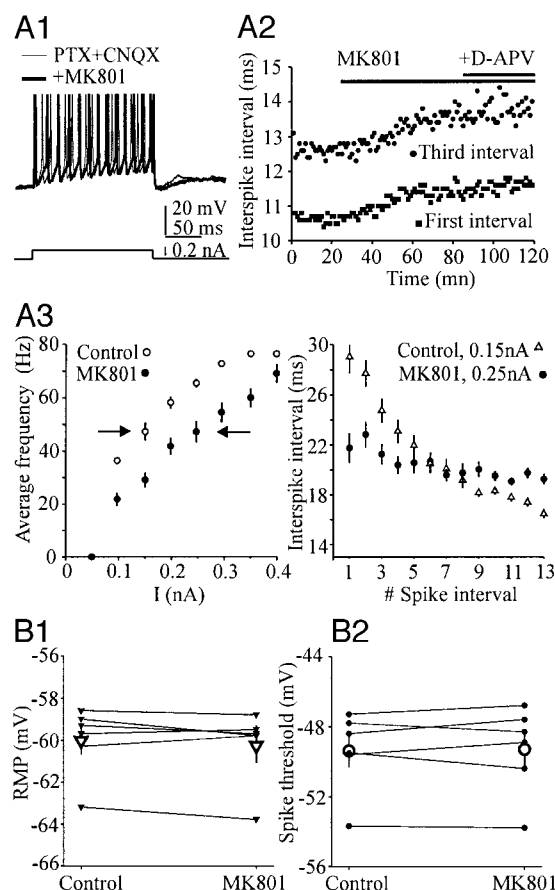


FIG. 8. Self-excitation exerts a positive feedback on MC activity. A1: self-excitation facilitates MC firing. Application of MK801 (40 μ M) for 20 min decreased the number of spikes evoked by a depolarizing current step (100 μ M PTX, 20 μ M CNQX, 0.8 mM Mg^{2+}). The 1st spikes were superimposed in both conditions (resting membrane potential: -59.7 vs. -59.5 mV; spike threshold: -47 vs. -46.8 mV). Experiments during which the membrane potential or the bridge balance compensation varied were discarded. A2: time course of the effects of MK801 (same cell as in A1). Subsequent application of 50 μ M D-APV had no effect. A3: the current-average frequency curve (left) during application of MK801 demonstrates that activation of NMDA autoreceptors increases cell excitability. Right: MK801 shapes MC's firing pattern. The distribution of the inter-spike interval was plotted as a function of the spike rank during a MC's discharge evoked by 2 depolarizing current pulses (0.15 nA in control; 0.25 nA in the presence of MK801). Current values were chosen (arrows on the left graph) to induce similar average firing frequency. In control condition (PTX, CNQX, and Mg^{2+}), self-excitation caused an acceleration of cell firing that was blocked by MK801. B1: the resting membrane potential (RMP) was not modified by the application of MK801 (quantification done in control conditions and 25 min after the beginning of the application of MK801; -60 \pm -0.6 mV vs. -60.2 \pm 0.8 mV, n = 6, P = 0.29, paired t -test). B2: MK801 did not change the spike threshold (1st spike: -49.4 \pm 0.9 mV vs. -49.3 \pm 1 mV (n = 6, P = 0.78, paired t -test).

8A3 (right) illustrates that MK801 also modified MCs' firing pattern, flattening the discharge rate as a function of time. These results indicate that the NMDA-mediated self-excitation acts as an excitatory feedback that shapes MC's own activity.

DISCUSSION

The goal of the present paper was to examine in more detail the mechanisms of self-excitation and its physiological role. We first demonstrate that olfactory bulb excitatory connections are not responsible for the slow-EPSP. The fact that intracel-

lular blockade of the spontaneous glutamate release deeply reduced the frequency of miniature NMDA-R-mediated synaptic currents in the same neuron directly implicates NMDA autoreceptors. However, in the experiments shown here, we cannot totally exclude the possibility of the contribution of glutamate release from neighboring MCs (Isaacson 1999). The paper also shows that, during self-excitation, there is a modest but significant activation of AMPA/kainate autoreceptors. These autoreceptors are located in part in the glomerular region of the primary dendrite while the major component of the slow-EPSP results from the activation of NMDA autoreceptors located on secondary dendrites. Finally, the study indicates that there is a frequency facilitation of self-excitation and that it may control the MC's firing in an activity-dependent manner.

Given the presence of intrinsic excitatory connections in olfactory bulb (see RESULTS), it was important to discard the possibility that the slow-EPSP was generated by conventional synaptic mechanisms. We were able to separate the two synaptic mechanisms by using an agonist of presynaptic metabotropic glutamate receptors and by examining the frequency of miniature NMDA currents after blockade of glutamate release in the recorded neuron. We considered also the respective contribution of primary and secondary dendrites in the generation of self-excitation. Indeed, the major component of the self-excitation results from an activation of glutamate receptors localized in MC secondary dendrites, indicating the important role of backpropagating action potentials in the MC integration of the signal. The coincidence of bursts of axonal action potentials and the self-excitation may, in turn, facilitate the generation of calcium and sodium action potentials in secondary dendrites depending on the level of dendrodendritic inhibition (Larkum et al. 1999). Finally, it has been recently shown that the distal primary dendrite can initiate mitral cell action potentials (Chen et al. 1997). In this context, it will be important to determine the potential role of dendritic action potentials evoked by activation of the olfactory nerve in the generation of self-excitation and, reciprocally, to examine the contribution of self-excitation to the regulation of distal dendritic impulses.

Here, we have shown that self-excitation is mediated in part by AMPA/kainate receptors. Given that one previous report (Isaacson 1999) did not mention this result, we discard, by using high doses of different NMDA-R antagonists, the possibility of an incomplete blockade of NMDA receptors. In the work of Isaacson, self-excitation was evoked with Ca currents, using cesium-gluconate-filled pipettes and tetrodotoxin. In our experiments, the size of the NMDA-R-mediated currents when evoked by Ca spikes in the absence of extracellular magnesium is very large in comparison with the amplitude of the AMPA-R-mediated currents. In that case, it was possible that the non-NMDA component was partially masked by the Ca currents/spikes. Indeed, when Na spikes evoked the slow current (with potassium gluconate-filled patch pipette), the rise time of the AMPA/kainate-R response was so fast that it was difficult to distinguish it from the end of the sodium current (partially clamped). Our result indicates that AMPA receptor subunits localized on MC dendrites (Montague and Greer 1999) have a physiological role. Thus self-excitation is not silent at the resting membrane potential since AMPA/kainate receptor-me-

diated EPSPs may unblock NMDA receptors. It will be important to determine whether AMPA and NMDA autoreceptors are co-localized in the neighborhood of the dendrodendritic synapses.

The duration of the CNQX/NBQX-sensitive component is long in comparison to the known kinetics of the AMPA receptors. Several reasons may explain this result. First, it is possible that there is also a contribution of kainate receptors in self-excitation since it has been shown that kainate receptor-mediated response present a prolong decay (Castillo et al. 1997). Second, dendrodendritic synapses are located on several sites of secondary dendrites, and backpropagating action potentials may induce a prolonged glutamate release by an activation of several release sites. Finally, we cannot exclude an imperfect voltage and space clamp of the glutamate receptor-mediated responses since MCs possess very long processes (the site of recording was in the soma).

The presence of an AMPA receptor-mediated response is surprising given the low affinity of the receptor for glutamate. It has been demonstrated that glutamate spillover may activate NMDA or metabotropic glutamate receptors that have a much higher affinity for glutamate than AMPA receptors (Kullmann and Asztely 1998). Given the results of models of glutamate diffusion (Clements 1996), the localization of AMPA receptors should be very close to the release sites (i.e., a distance smaller than 400 nm) (see Holmes 1995). Increase in glutamate concentration by release of glutamate from neighboring sites (see, for example, Scanziani et al. 1997) located on the MC dendrites or a delayed clearance of the neurotransmitter caused by some obstacle to the neurotransmitter diffusion in the extracellular space could also contribute to the AMPA receptor activation. In support of these latter possibilities is the relatively slow time course of the decay of the AMPA receptor component that could be in part due to a prolonged presence of glutamate (Barbour et al. 1994).

We found a modulation of MC excitability by self-excitation, suggesting a precise role of this phenomenon for the temporal coding of odor signals. It is now well established that sensory neurons lack response selectivity for odor ligands and present a relatively high level of spontaneous activity (Duchamp-Viret et al. 1999; Malnic et al. 1999). In contrast, MCs have a much narrower tuning curve than sensory neurons (Duchamp-Viret and Duchamp 1997; Mori and Yoshihara 1995), and the cellular interactions underlying the increase in selectivity in the olfactory bulb have yet to be determined. Self-excitation may contribute to an increase in the signal-to-noise (S/N) ratio by amplifying active inputs from sensory neurons with an excitatory feedback mechanism. The behavior of such an amplifier has been extensively analyzed in models of recurrent excitation in cerebral cortex (Douglas et al. 1995; Somers et al. 1995), and it has been shown that this could be a powerful mechanism for improving the response selectivity of cortical neurons to noisy inputs. Indeed, the effect of NMDA autoreceptor activation on the slope of the average frequency curve (see Fig. 8A3) suggests an increase in the S/N ratio for the specific set of MCs that are most activated, as in these models. Together with the disinaptic inhibition, self-exci-

tation exerts a push-pull regulation of the spike discharge that may contribute to the coding of olfactory inputs.

REFERENCES

- ADLER EM, AUGUSTINE GJ, DUFFY SN, AND CHARLTON MP. Alien intracellular calcium chelators attenuate neurotransmitter release at the squid giant synapse. *J Neurosci* 11: 1496–1507, 1991.
- ARONIADOU-ANDERJASKA V, ENNIS M, AND SHIPLEY MT. Dendrodendritic recurrent excitation in mitral cells of the rat olfactory bulb. *J Neurophysiol* 82: 489–494, 1999.
- ASZTELY F, ERDEMLI G, AND KULLMANN DM. Extrasynaptic glutamate spillover in the hippocampus: dependence on temperature and the role of active glutamate uptake. *Neuron* 18: 281–293, 1997.
- BARBOUR B, KELLER BU, LLANO I, AND MARTY A. Prolonged presence of glutamate during excitatory synaptic transmission to cerebellar Purkinje cells. *Neuron* 12: 1331–1343, 1994.
- BEKKERS JM. Neurophysiology: are autapses prodigal synapses? *Curr Biol* 8: 52–55, 1998.
- BISCHOFBERGER J AND JONAS P. Action potential propagation into the presynaptic dendrites of rat mitral cells. *J Physiol (Lond)* 504: 359–365, 1997.
- BORST JG AND SAKMANN B. Calcium influx and transmitter release in a fast CNS synapse. *Nature* 383: 431–434, 1996.
- CASTILLO PE, MALENKA RC, AND NICOLL RA. Kainate receptors mediate a slow postsynaptic current in hippocampal CA3 neurons. *Nature* 388: 182–186, 1997.
- CHEN WR, MA M, JIA C, AND SHEPHERD GM. Roles of action potential propagation, pre- and postsynaptic NMDA receptors in the activation of olfactory dendrodendritic reciprocal synapses. *Soc Neurosci Abstr* 24: 321, 1998.
- CHEN WR, MIDTGAARD J, AND SHEPHERD GM. Forward and backward propagation of dendritic impulses and their synaptic control in mitral cells. *Science* 278: 463–467, 1997.
- CLEMENTS JD. Transmitter timecourse in the synaptic cleft: its role in central synaptic function. *Trends Neurosci* 19: 163–171, 1996.
- CONN PJ AND PIN JP. Pharmacology and functions of metabotropic glutamate receptors. *Annu Rev Pharmacol Toxicol* 37: 205–237, 1997.
- DOUGLAS RJ, KOCH C, MAHOWALD M, MARTIN KA, AND SUAREZ HH. Recurrent excitation in neocortical circuits. *Science* 269: 981–985, 1995.
- DUCHAMP-VIRET P, CHAPUT MA, AND DUCHAMP A. Odor response properties of rat olfactory receptor neurons. *Science* 284: 2171–2174, 1999.
- DUCHAMP-VIRET P AND DUCHAMP A. Odor processing in the frog olfactory system. *Prog Neurobiol* 53: 561–602, 1997.
- HOLMES WR. Modeling the effect of glutamate diffusion and uptake on NMDA and non-NMDA receptor saturation. *Biophys J* 69: 1734–1747, 1995.
- ISAACSON JS. Glutamate spillover mediates excitatory transmission in the rat olfactory bulb. *Neuron* 23: 377–384, 1999.
- ISAACSON JS AND STROWBRIDGE BW. Olfactory reciprocal synapses: dendritic signaling in the CNS. *Neuron* 20: 749–761, 1998.
- JAHR CE AND NICOLL RA. An intracellular analysis of dendrodendritic inhibition in the turtle in vitro olfactory bulb. *J Physiol (Lond)* 326: 213–234, 1982.
- KAMIYA H AND OZAWA S. Dual mechanism for presynaptic modulation by axonal metabotropic glutamate receptor at the mouse mossy fibre-CA3 synapse. *J Physiol (Lond)* 518: 497–506, 1999.
- KULLMANN DM AND ASZTELY F. Extrasynaptic glutamate spillover in the hippocampus: evidence and implications. *Trends Neurosci* 21: 8–14, 1998.
- LANGER SZ. 25 years since the discovery of presynaptic receptors: present knowledge and future perspectives. *Trends Pharmacol Sci* 18: 95–99, 1997.
- LARKUM ME, ZHU JJ, AND SAKMANN B. A new cellular mechanism for coupling inputs arriving at different cortical layers. *Nature* 398: 338–341, 1999.
- MACEK TA, WINDER DG, GEREAU RW IV, LADD CO, AND CONN PJ. Differential involvement of group II and group III mGluRs as autoreceptors at lateral and medial perforant path synapses. *J Neurophysiol* 76: 3798–3806, 1996.
- MALNIC B, HIRONO J, SATO T, AND BUCK LB. Combinatorial receptor codes for odors. *Cell* 96: 713–723, 1999.
- MARTINEZ DP AND FREEMAN WJ. Periglomerular cell action on mitral cells in olfactory bulb shown by current source density analysis. *Brain Res* 308: 223–233, 1984.
- MONTAGUE AA AND GREER CA. Differential distribution of ionotropic glutamate receptor subunits in the rat olfactory bulb. *J Comp Neurol* 405: 233–246, 1999.
- MORI K AND YOSHIHARA Y. Molecular recognition and olfactory processing in the mammalian olfactory system. *Prog Neurobiol* 45: 585–619, 1995.
- NICOLL RA. Recurrent excitation of secondary olfactory neurons: a possible mechanism for signal amplification. *Science* 171: 824–826, 1971.
- NICOLL RA AND JAHR CE. Self-excitation of olfactory bulb neurones. *Nature* 296: 441–444, 1982.
- NOWYCKY MC, MORI K, AND SHEPHERD GM. GABAergic mechanisms of dendrodendritic synapses in isolated turtle olfactory bulb. *J Neurophysiol* 46: 639–648, 1981a.
- NOWYCKY MC, MORI K, AND SHEPHERD GM. Blockade of synaptic inhibition reveals long-lasting synaptic excitation in isolated turtle olfactory bulb. *J Neurophysiol* 46: 649–658, 1981b.
- PETRALIA RS, WANG YX, AND WENTHOLD RJ. The NMDA receptor subunits NR2A and NR2B show histological and ultrastructural localization patterns similar to those of NR1. *J Neurosci* 14: 6102–6120, 1994a.
- PETRALIA RS, YOKOTANI N, AND WENTHOLD RJ. Light and electron microscope distribution of the NMDA receptor subunit NMDAR1 in the rat nervous system using a selective anti-peptide antibody. *J Neurosci* 14: 667–696, 1994b.
- POUZAT C AND MARTY A. Autaptic inhibitory currents recorded from interneurons in rat cerebellar slices. *J Physiol (Lond)* 509: 777–783, 1998.
- PRICE JL AND POWELL TP. The mitral and short axon cells of the olfactory bulb. *J Cell Sci* 7: 631–651, 1970.
- RALL W AND SHEPHERD GM. Theoretical reconstruction of field potentials and dendrodendritic synaptic interactions in olfactory bulb. *J Neurophysiol* 31: 884–915, 1968.
- RALL W, SHEPHERD GM, REESE TS, AND BRIGHTMAN MW. Dendrodendritic synaptic pathway for inhibition in the olfactory bulb. *Exp Neurol* 14: 44–56, 1966.
- SAH P, HESTRIN S, AND NICOLL RA. Tonic activation of NMDA receptors by ambient glutamate enhances excitability of neurons. *Science* 246: 815–818, 1989.
- SALIN PA AND CHARPAK S. Self-excitation of mitral cells in the rat olfactory bulb: role of NMDA autoreceptor. *Soc Neurosci Abstr* 24: 321, 1998.
- SCANZIANI M, SALIN PA, VOGT KE, MALENKA RC, AND NICOLL RA. Use-dependent increases in glutamate concentration activate presynaptic metabotropic glutamate receptors. *Nature* 385: 630–634, 1997.
- SCHOPPA NE, KINZIE JM, SAHARA Y, SEGERSON TP, AND WESTBROOK GL. Dendrodendritic inhibition in the olfactory bulb is driven by NMDA receptors. *J Neurosci* 18: 6790–6802, 1998.
- SOMERS DC, NELSON SB, AND SUR M. An emergent model of orientation selectivity in cat visual cortical simple cells. *J Neurosci* 15: 5448–5465, 1995.
- VAN DEN POL AN. Presynaptic metabotropic glutamate receptors in adult and developing neurons: autoexcitation in the olfactory bulb. *J Comp Neurol* 359: 253–271, 1995.
- WELLIS DP, SCOTT JW, AND HARRISON TA. Discrimination among odorants by single neurons of the rat olfactory bulb. *J Neurophysiol* 61: 1161–1177, 1989.